# The J-Box Problem

Presented by
Dr Andy Banks, Acordis

Study Group contributors

| | | | |
|---|---|---|---|
| David Allwright | Andy Banks | John Byatt-Smith | Jon Chapman |
| Paul Dellar | Alistair Fitt | Rob Hinch | John Hinch |
| Sam Howison | Marvin Jones | John Ockendon | Hilary Ockendon |
| David Parker | Colin Please | Domingo Salazar-Gonzalez | Jihong Wang |
| Rex Westbrook | | | |

This report was prepared by Colin Please, Marvin Jones and David Allwright.

# 1 Introduction

The study group was presented with the problem of determining the behaviour of a web of wet cellulose fibres — called a *tow* — as it passes through part of the manufacturing process shown diagrammatically in Figure 1. The name of the problem derives from the fact that on its passage down the production line the tow passes through a J-shaped box, whose purpose is to provide a buffer where the tow is stored long enough and hot enough for certain chemical reactions to take place, mainly concerned with giving the right quality to the fibre surface. (The production line in fact involves *two* J-boxes, one containing wet tow, the other dry, and we are here entirely concerned with the first of these, the *wet* J-box.)

Three aspects of the tow behaviour were proposed for investigation:

1. What is the mechanical behaviour of the tow within the J-box ? Specifically, how do the time spent within the J-box and the shape of the tow outlet column depend on the J-box geometry, tow density and compressibility, flow rate, friction coefficients *etc.*

2. What is the temperature history, and hence the chemical history, of the tow within the J-box ?

3. Why do dislocations and loops occur within the tow ?

We first give typical parameters and other details of the process, and then further details of these three questions.

## 1.1 Parameter ranges and typical values

The individual cellulose fibres are about 10 $\mu$m in diameter when dry, and are formed in ribbons called *ends*, each containing about $10^4$ fibres. The entire tow band may consist of 20–100–200 ends (*ie* in the range 20–200, with 100 as a typical value). These form a web of width $c$=0.2–1.0–2.0 m and perhaps 5 mm thick. The speed $U_*$ at which the tow passes along the production line may be 10–50–100 m/min. Before entering the wet J-box, the

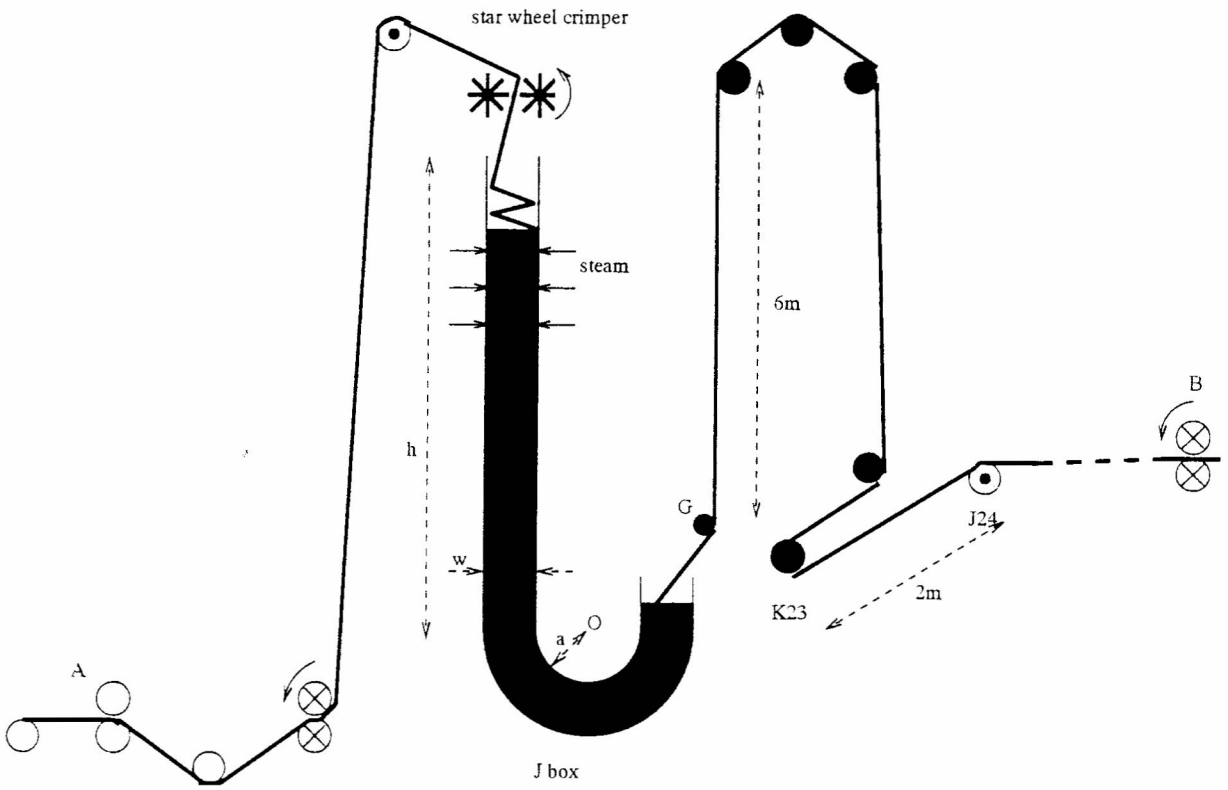


Figure 1: Schematic diagram of the part of the production line including the wet J-box.
Tow moves from left to right, entering at A, leaving at B.
Solid circles denote guides (non-rotating).
Circles with a central dot denote rollers (freely rotating).
Circles containing a cross are nips (driven in direction of arrows).

tow passes over rollers and through the star-wheel crimper, which puts a crimp wavelength 1–4–10 cm into the tow. At entry to the wet J-box, the tow may have a moisture content of 100–180–250%, *ie* 100–180–250 gm of water per 100 gm of dry fibre. The tow temperature at entry to the wet J-box may be 20–100°C. The dimension of the J-box perpendicular to the plane drawn in Figure 1 is equal to the width $c$ of the tow. The J-box inlet duct width $w$ is 0.3–0.5–1.0 m, with the aspect ratio $c : w$ typically 2:1. The inlet duct height $h$ is 1–4 m. The bend of the J is semicircular with inner radius $a$=0.1–0.4 m, and outer radius $b = a + w$. In the plane of motion drawn in Figure 1 we shall use $(x, y)$ as horizontal and vertical Cartesian coordinates, with origin at the centre O of the semicircular part of the J. We shall also use polar coordinates $(r, \theta)$ in this plane, and $z$ will be the coordinate perpendicular to this plane.

The tow can be laid back and forth into the J-box inlet duct as shown in Figure 1, a process called *plaiting*, (pronounced to rhyme with "waiting"), with the intention of filling uniformly across the entire width $w$ of the J-box. The plaiting arm does a complete cycle (distance $2w$) in $t_p = 9.1$ seconds. Alternatively the plaiting arm can be switched off and

the tow just allowed to fall naturally onto the top of the tow inlet column.

The rate of dry steam injection may be 500–1500 kg/hr, the steam being supplied to the upper part of the inlet duct by an array of pipes. The tow is heated to 100°C by this, and the condensate is absorbed by the tow. (There is a tap at the bottom of the J-box, but when it is opened, no water emerges.)

The column of tow in the inlet duct moves down and compresses under its own weight. (The density of the bulk material at the bottom of the J may be around 400 kg/m$^3$.) The tow rotates round the bend at the bottom, and forms a column in the outlet duct. The time of passage through the box may be 15 minutes. From the bed of tow at the top of the outlet column, the tow is pulled out and passed over a further series of rollers and then into other processing parts of the plant.

## 1.2 Tow mechanics in the wet J-box

Acordis have a mathematical model of the flow through the J-box. This model is needed in order to understand how the residence time in the J-box depends on the inlet column height, the friction coefficient between the tow and the box, the speed, density *etc.* This existing model is 1-dimensional, with the tow density and pressure being treated as functions of distance along the J-box centreline.

However, some features of the process are not 1-dimensional, in particular the column of tow in the outlet duct is not always as drawn in Figure 1. Often there is a gap between the tow and the inner duct wall, and sometimes the bed (upper surface of the tow outlet column) is tilted, as in Figure 2.

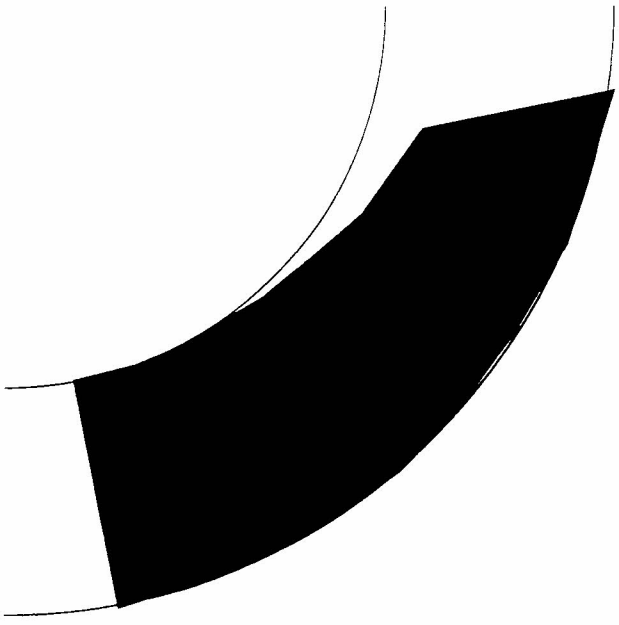

Figure 2: Gap and tilt of the outlet column.

The gap itself is not a concern, but the tilting is, because the tow can slip or roll down the slope, and this causes snagging when the tow is pulled off. There is therefore a need for a 2-dimensional model of the flow of tow through the J-box.

### 1.3 Temperature distribution in the J-box

Measurements taken by a thermocouple dropped onto the centre of the inlet column, and recovered off the outlet bed, show that the temperature there rises rapidly to 100°C and remains at that value until the exit. However, is that behaviour uniform across the cross-section of the duct ? How quickly does the steam penetrate the full volume of the tow ? These questions matter because the time-temperature history of a given part of the tow determine whether or not the chemical processes reach the desired state.

### 1.4 Dislocations and loops

Downstream of the J-box, the tow is sometimes not continuous across the width $0 \leq z \leq c$, but has a *slit* at some position $z_0$. If a blue line is marked straight across the width of the tow ($0 \leq z \leq c$) before entry to the J-box, then it is observed that downstream of the J-box this line may be *discontinuous* across such a slit, perhaps by as much as a metre. This kind of fault is referred to as a *dislocation.* It can happen that there are a number of these dislocations, so the blue line comes out as a number of staggered segments.

Another kind of fault is sometimes observed, in which at some part of the production line a strip $z_0 \leq z \leq z_1$ of the tow has extra length, and so hangs down below the general line of the tow, forming what is called a *loop.*

The cause of these dislocations and loops was put to the study group, along with certain observations about their occurrence.

### 1.5 Outline of contents of report

The second, thermal, problem was not considered in any detail and so this report concentrates on results from work done to understand the first and third.

There were two separate approaches to the problem. The first attempted to investigate the possible sources of dislocations and concentrated on the movement of the tow within the J-box itself while the second attempted to explain the appearance of the loops and other variations in tension in the tow and concentrated on the tow where it passed over rollers.

## 2 Dislocation creation within the J-box

A number of different mechanisms were considered as possible sources for creating dislocations. These included :

- Uneven removal of the web due to "scrumpling" during the plaiting process and tangling when the web is removed.

- Uneven moisture content of the web near the exit, particularly due to "pillowing", and resulting uneven stretching of the fibres.
- "Fracturing" of carefully laid out tow within the J-box due to uneven flow resulting in tangling between different parts.

Ideas relating to the first of these is presented in the last part of this section while work on the other two primarily concentrated on determining how the tow passed through the J-box and is presented next.

## 2.1 Movement of tow within the J-box

The main aim of the flow modelling was to give insight into the movement of the tow. In particular this should indicate how the tilt of the exit bed could be controlled, give insight into the the importance and effect of the separation of the bed from the inner edge of the J-box and give a basis for understanding any fracturing.

The flow was expected to contain two main regimes:

1. approximately vertical plug flow with the tow steadily compressing under the "fibrostatic" stresses induced by gravity.
2. approximately azimuthal flow around the lower part of the J-box

Each of these parts is described by a rigid body motion and so the critical question in determining the flow is to identify how the material deforms as it passes from one regime to the other.

There was significant uncertainty as to what type of material the packed tow is best modelled by. The following observations where thought to be relevant:
1) when wet tow is freely laid down, and compressed vertically, most of the strain induced is *not* recovered when the compression is removed.
2) The plaiting process is very irregular and so, even when compressed vertically, the tow still contains significant voids.
The flow is driven by the gravitation head induced in the vertical section, is slowed by internal friction and other losses within the material and by friction with the walls. The flow is so slow that inertia effects are negligible.

Various material properties were considered as possible candidates for the flow and each is described below.

### 2.1.1 Incompressible deformable blocks

This is a highly simplified model of the flow with the material taken to change behaviour from the vertical to the azimuthal behaviour instantaneously at the start of the curve in the J section. There must be a change in shape to accommodate this, from a rectangle to a sector of an annulus, as shown in the left pair of diagrams in Figure 3. If the material is incompressible, there must be some radial flow in the material, from the inner edge towards

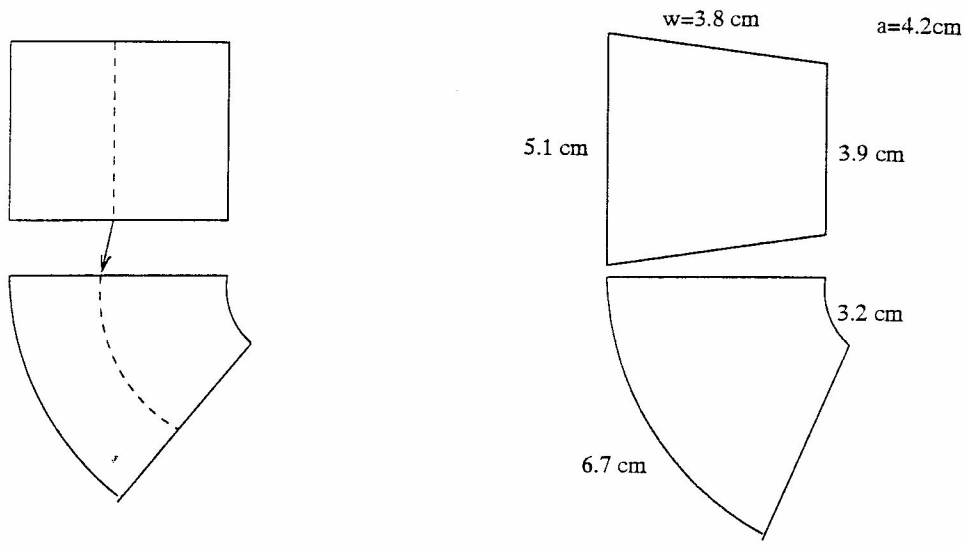


Figure 3: Change in geometry of a block of material. On the left is the ideal change from a rectangle to a sector of an annulus, with the radial displacement of the dotted line necessary to preserve areas. On the right are approximate measured values for a block of material in the model J-box.

the outer edge, in order to conserve the volume of material. In fact, material initially at radius $r$ $(a \leq r \leq b)$ must move out to radius $\sqrt{(a+b)r - ab}$ in order for volume to be conserved. The maximum radial displacement is for $r = \frac{1}{2}(a+b)$, and if for instance $b/a = 2$ then material initially on the centreline $r = 1.5a$ moves out to $r = 1.58a$. It would be very interesting to know whether these displacements occur in the real J-box, or whether the compressibility of the material allows the motion to be more nearly circumferential.

We attempted to measure such motion in the small model J-box, pushing relatively dry tow through, identifying a suitable small block in the inlet column, and measuring it when it had entered the bend. However, it was not possible to measure radial displacements without better equipment. The radial compression of the material at $r = a$ and expansion at $r = b$ were very marked though, and approximate measured dimensions are given in the right hand pair of figures in Figure 3.

### 2.1.2 Compressible elasticity

A purely elastic model of the deformation of the material will result in any strain being recoverable. Although this is possible in theory — think of a column of very soft rubber being pushed through the J-box — observation of both the model J-box and the real J-box indicates that it is not what really happens. In particular, after a block of material has been round the bend, it has acquired the curvature of the bend, and if it is allowed to continue without being pulled off, it curves over in a continuation of the curve of the J-box shape. So this model is thought to be unrepresentative of the behaviour.

### 2.1.3 Incompressible plasticity

Some type of permanent deformation to the material is required and a possible model is to use conventional plasticity theory to predict the flow. A suitable reference for plasticity is the book by Hill [1]. An elastic-plastic model would treat the material as behaving elastically until the appropriate yield criterion is reached, and then behaving plastically, *ie* flowing under the applied stress. However, since the plastic deformation in such a model generally far exceeds the elastic, the simplification is normally made of treating the elastic region as rigid, resulting in what is called a rigid-plastic model. In this model the motion is rigid body where the total stress (to be defined later) is below the yield stress $\sigma_0$ of the material and otherwise the stress is at the yield criterion.

In the case of the flow through the J-box, the actual region where plastic flow is occurring cannot easily be determined: presumably we shall have rigid body motion in the inlet duct, then some yield boundary where the material enters a region of plastic flow, then a recovery boundary where it reverts to rigid body motion and the total stress is below $\sigma_0$ again. Plastic flow models like this need to be completed by a flow law for those regions where the yield criterion has been reached. The simplest such law is to take that used for flow of metals, in which the symmetric part of the velocity gradient tensor is taken to be proportional to the deviatoric part of the stress tensor. In the analysis here, we shall also treat the whole motion as two-dimensional.

Hence in regions where the material has yielded we write the stress tensor $\sigma$ as

$$\sigma_{ij} = -p\delta_{ij} + T_{ij} \tag{1}$$

where $p = -\frac{1}{2}(\sigma_{11} + \sigma_{22})$ is the mean hydrostatic pressure, and the deviatoric part $T_{ij}$ of the stress satisfies $T_{11} + T_{22} = 0$. If we introduce for convenience

$$\tau_1 = T_{11} = -T_{22} \qquad \tau_2 = T_{12} = T_{21} \tag{2}$$

then the von Mises yield criterion is that

$$\tau_1^2 + \tau_2^2 = \sigma_0^2, \tag{3}$$

where $\sigma_0$ is the yield stress of the material. (If a sample of the material is subjected to simple shear, so $\tau_1 = 0$, then $\sigma_0$ is the value of $\tau_2$ at which yield occurs. The above criterion generalizes this in a way that is rotationally invariant, and one can think of the total stress $\sqrt{\tau_1^2 + \tau_2^2}$ as the shear stress that is trying to cause plastic flow.)

Taking the velocities in the $x$ and $y$ directions as $u$ and $v$ respectively the flow law for the material can be written as

$$\tau_1 = T_{11} = \lambda u_x, \tag{4}$$

$$\tau_2 = T_{12} = \lambda \frac{1}{2}\left(u_y + v_x\right), \tag{5}$$

$$-\tau_1 = T_{22} = \lambda v_y. \tag{6}$$

(These automatically ensure that the incompressibility condition $u_x + v_y = 0$ is satisfied.) In view of these equations, it is natural to think of $\lambda$ as an effective viscosity, but it must be borne in mind that it is *not* a material parameter: its value will vary with position, and it must result in flow velocities that are compatible with the rigid-body velocities on the boundaries of the plastic region.

The force balance equations (ignoring the inertial terms) are

$$p_x = \tau_{1x} + \tau_{2y}, \tag{7}$$

$$p_y = \tau_{2x} - \tau_{1y} - \rho g \ . \tag{8}$$

This is a hyperbolic system of equations and can be solved using appropriate methods. To make progress analytically, we write

$$\tau_1 = \sigma_0 \sin\phi, \quad \tau_2 = \sigma_0 \cos\phi \tag{9}$$

and the equations then have two families $C_1$ and $C_2$ of characteristics, (which are orthogonal in this case) and Riemann invariants:

$$C_1: \quad dy/dx = \cot(\phi/2), \quad p + \rho g y + \sigma_0 \phi = \text{constant} \tag{10}$$

$$C_2: \quad dy/dx = -\tan(\phi/2), \quad p + \rho g y - \sigma_0 \phi = \text{constant}. \tag{11}$$

Some simple flows can then be considered in the usual way by considering cases where one of the invariants is constant *throughout the flow* (not just constant along each characteristic). However, the details of this were not worked out at the Study Group.

### 2.1.4 Compressible plasticity

It was noted that there are numerous voids in the material and that these may contribute significantly to the flow especially since the material is observed to separate from the inner edge of the J-box and this might be taken to be due to compression of the tow. The analysis of the problem is similar to the incompressible case but there are additional difficulties. The first of these relates to the usual compressible flow problem of accounting for the stress due to compression. There was some uncertainty as to whether an isotropic compression in three dimensions should result in no stress or if a purely two dimension compression should suffice. The following assume the two dimensional case and the 3-D version merely needs the constants altering. We assume that the density is a fixed function of the pressure $\rho = \rho(p)$ and note that such a law does not exclude recovery of the material when the compression is removed so further refinements relating to maximum pressure encountered by a flow particle may be necessary later. The flow law has to be modified, and we assume that in the previous relations the velocity gradient tensor must now be replaced by its deviatoric part, so

$$\tau_1 = T_{11} = -T_{22} = \lambda\left(u_x - \frac{1}{2}(u_x + v_y)\right) = \lambda\frac{1}{2}(u_x - v_y) \tag{12}$$

$$\tau_2 = T_{12} = \lambda\frac{1}{2}(u_y + v_x) \ . \tag{13}$$

To this system we must explicitly add the mass conservation equation (which was previously automatically satisfied)

$$(\rho u)_x + (\rho v)_y = 0 \, . \tag{14}$$

To make progress analytically with this, one would again have to look at simple flows, where one of the Riemann invariants is constant.

## 2.2 Scrumpling and tangling

The seed of the plaiting arm is much less than the drop speed of the tow into the J-box. In fact if $w = 0.5$ m then the tip of the plaiting arm (moving a distance $2w$ in $t_p = 9.1$ s) has a speed 1.1 m/s, whereas the tow velocity can be 50–100 m/min, *ie* 7.5–15 times greater. The observations of the plaiting of the tow in the *dry* J-box show that this speed mismatch causes the tow to scrumple when it lands on the inlet bed. It is anticipated that the same must happen in the wet box. This scrumple is on a length scale intermediate between the box size ($w$, of order 50cm) and the crimp length (4cm). It was noted that this scrumpling could be greatly reduced and the tow laid in the J-box move uniformly if either the plaiting speed was increased to be much closer to the drop speed or the plaiting system was vibrated at a frequency close to the scrumple frequency so that the scrumpling was then induce to be uniform across the web. When the tow is removed from the J-box the edges of the various scrumpled sections have the possibility of connecting together and hence pulling up web out of sequence with when it was laid down. Such out of sequence behaviour could occur on a scrumple length scale (perhaps 10cm) or on a plaiting layer by plaiting layer length scale (some 250cm). This might explain the rather quantised distances that appear to occur across a dislocation in the "blue line" experiments.

The formation of a "pillow" when the exit bed gets to a high angle of tilt was considered as a possible mechanism for creating dislocations. This is shown diagrammatically in Figure 4

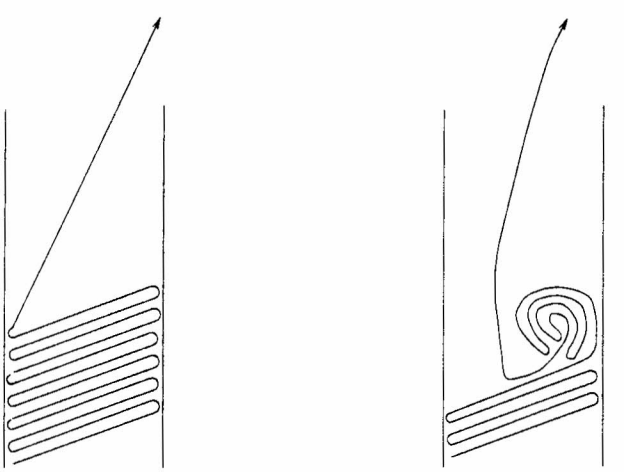

Figure 4: If the exit tow bed becomes tilted, as on the left, it is possible that part of the tow can roll down the slope, forming a pillow as on the right.

This pillowing could be extreme in the form of overturning of the entire exit flow or more minor being a collapse of the tow towards the inner edge of the J-box. In particular any pillow will create large changes in the tension required to pull the web from the exit of the J-box. Those tension variations will persist downstream as far as the nip (B in Figure 1) where the tow is being pulled. Since that may be 30 m away, and tow can stretch by 5% elastically, there is certainly scope for considerable misalignment to arise once the tow has slit longitudinally. When a dislocation has occurred across such a slit, continual slit formation is required to maintain it. Alternatively, if for some reason a slit moves across the tow, then the region traversed contains extra length and the extra material there can form a loop.

An alternative method of loop formation is if one group of ends is pulled out of the J-box early, by having tangled with earlier ends either side of them.

# 3 Tow Dynamics

In addition to the J-Box problem another problem was presented in the brief supplied by Acordis. This problem was concerned with the general dynamics of a length of tow moving through a tow handling system consisting of a number of guides, rollers, and nips. Certain specific goals were stated in the brief and included the following:

- The validation or otherwise of a pre-existing 1D steady state model, developed by Acordis, in the form of an energy balance.
- The development of a 1D unsteady model for the motion of the tow band through the handling system which would incorporate more general tow properties, such as variable elastic modulus, include the frictional forces at the guides, rollers, and nips and allow the use of more general time dependent boundary conditions.

It was mentioned that a 2D model which allowed cross-tow variations to be supported by inter-fibre, or inter-end, frictional forces would be ideal.

We begin with the second of these goals by developing a 1D unsteady model for the movement of the tow band through the tow handling system. We model the tow as a 1D elastic fibre whilst letting the elastic modulus of the tow vary as a function of density. Usually such a model would be considered within a Lagrangian framework and evolution equations for the position of the particles which make up the fibre would be derived. However, due to the nature of the boundary conditions at the guides, rollers, and nips in the handling system, and the fact that we are primarily interested in the steady state solution of such a model, it seemed more natural to deal with the problem within an Eulerian framework. Therefore, we consider the motion of a 1 dimensional elastic tow band in 2 dimensional space as follows.

## 3.1 Problem Formulation

Firstly, it is important, within the Eulerian framework, to recognise the difference between the shape of the tow band and the position of the material points which make up the tow

band. Having noted this difference we parameterise points on the tow band shape with arc length, $s$, from the J-box position $(x_j(t), y_j(t))$ which is of course a point on the tow band shape. The shape of the tow band at successive times $t$ can then be described completely by the angle its tangent vector makes with the horizontal at each point $s$ along its length. This angle is denoted $\theta(s,t)$. As a result the horizontal and vertical co-ordinates of a point on the tow band shape, parameterised by $s$ and $t$, are written as

$$x(s,t) = x_j(t) + \int_0^s \cos\theta(\xi,t)\, d\xi, \tag{15}$$

$$y(s,t) = y_j(t) + \int_0^s \sin\theta(\xi,t)\, d\xi, \tag{16}$$

respectively.

We not only allow the shape of the tow band to evolve in space and time but also allow the particles which make up the tow band to flow tangentially along the tow band shape with speed $u(s,t)$. Since the tow is modelled as an elastic fibre the mass per unit length of the tow, denoted $\rho(s,t)$, must also be allowed to vary along the length of the tow band and in time. Finally, the tension within the tow band, denoted $T(s,t)$, is included and is allowed to vary along the length of tow band and in time. We include gravity in the problem and the frictional forces encountered at the guides, nips, and rollers are also incorporated later on. See Figure 5.

Conservation of mass and tangential and normal momentum considerations then yield the governing partial differential equations

$$\frac{\partial\rho}{\partial t} + u\frac{\partial\rho}{\partial s} + \rho\frac{\partial u}{\partial s} = 0, \tag{17}$$

$$\cos\theta\frac{\partial^2 x}{\partial t^2} + \sin\theta\frac{\partial^2 y}{\partial t^2} + \frac{\partial u}{\partial t} + u\frac{\partial u}{\partial s} = \frac{\lambda}{\rho}\frac{\partial T}{\partial s} - \gamma\sin\theta, \tag{18}$$

$$\cos\theta\frac{\partial^2 y}{\partial t^2} - \sin\theta\frac{\partial^2 x}{\partial t^2} + 2u\frac{\partial\theta}{\partial t} + u^2\frac{\partial\theta}{\partial s} = \frac{\lambda T}{\rho}\frac{\partial\theta}{\partial s} - \gamma\cos\theta, \tag{19}$$

respectively, where we have non-dimensionalised the equations based on the typical tow band length $S_*$, the unstressed tow density $\rho_*$, the typical tow band velocity $U_*$, and the unstressed elastic modulus of the tow $E_*$ in the correct units. The non-dimensional parameters $\lambda$ and $\gamma$ are defined as the ratios

$$\lambda = \frac{E_*}{\rho_*^2 U_*^2} \quad \text{and} \quad \gamma = \frac{gS_*}{U_*^2}.$$

We require one additional relation to close the system and this comes in the form of a constitutive relationship between the tension $T(s,t)$ and the linear density $\rho(s,t)$. We use a non-linear elastic model for the tow band and hence

$$T(\rho) = \int_\rho^1 \frac{E(\xi)}{\xi^2} d\xi, \tag{20}$$

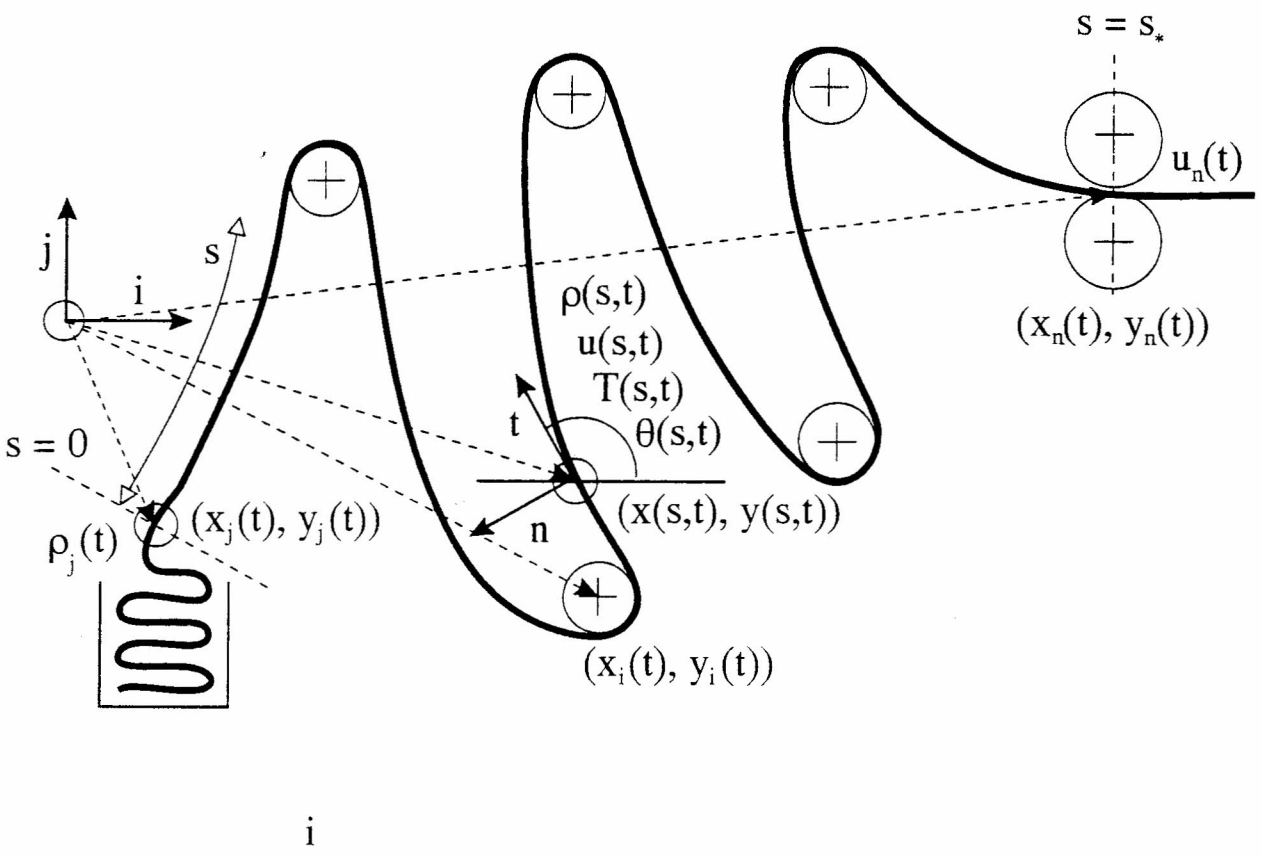


Figure 5: A tow handling system consisting of a J-box exit, a nip roller, and a number of intermediate guides and rollers. The tow band shape is parameterised by the arc length $s$ and described by the tangent angle $\theta(s,t)$, its cartesian coordinates $(x(s,t), y(s,t))$. Tow band density is denoted $\rho(s,t)$, tension denoted $T(s,t)$, and tangential velocity $u(s,t)$.

where $E(\rho)$ defines the elastic modulus of the tow as a function of its linear density $\rho(s,t)$ and is assumed known.

In order to solve the system of equations (15)-(20) we expect to prescribe initial conditions on the tow density, velocity, and shape at time $t = 0$ and so

$$\left.\begin{array}{rcl} \rho(s,0) & = & \rho_0(s) \\ u(s,0) & = & u_0(s) \\ \theta(s,0) & = & \theta_0(s) \\ \frac{\partial\theta}{\partial t}(s,0) & = & \omega_0(s) \end{array}\right\}, \tag{21}$$

a boundary condition on the density at the exit to the J-Box and so

$$\left.\begin{array}{rcl} \rho(0,t) & = & \rho_j(t) \\ x(0,t) & = & x_j(t) \\ y(0,t) & = & y_j(t) \end{array}\right\}, \tag{22}$$

and a free boundary condition on the take up velocity at the final nip roller and so

$$\left.\begin{array}{rcl} u(s_*(t),t) & = & u_n(t) \\ x(s_*(t),t) & = & x_n(t) \\ y(s_*(t),t) & = & y_n(t) \end{array}\right\}. \tag{23}$$

The function $s = s_*(t)$ denotes the total length of the shape of the tow band within the handling system at time $t$ and must be found as part of the solution.

## 3.2 Steady Tow Dynamics

Since the ideal mode of operation for the tow handling system is presumably the steady state situation we now go on to consider the steady state solution of the system of equations (15)-(23).

The steady state equations take the following form

$$x(s) = x_j + \int_0^s \cos\theta(\xi)\, d\xi, \tag{24}$$

$$y(s) = y_j + \int_0^s \sin\theta(\xi)\, d\xi, \tag{25}$$

$$u\frac{du}{ds} = \frac{\lambda}{\rho}\frac{dT}{ds} - \gamma\sin\theta, \tag{26}$$

$$u^2\frac{d\theta}{ds} = \frac{\lambda T}{\rho}\frac{d\theta}{ds} - \gamma\cos\theta, \tag{27}$$

$$T(\rho) = \int_\rho^1 \frac{E(\xi)}{\xi^2} d\xi, \tag{28}$$

with the additional constraint that

$$\rho u = q, \tag{29}$$

where $q$ is the unknown constant mass flow rate.

Some simplification of the system of equations (24)-(29) can be made by eliminating the tension $T(s)$ and the velocity $u(s)$ using equations (28) and (29). If we do this we obtain the coupled system of ordinary differential equations

$$\frac{d\rho}{ds} = \frac{\gamma\rho^3 \sin\theta}{q^2 - \lambda E(\rho)}, \tag{30}$$

$$\frac{d\theta}{ds} = -\frac{\gamma\rho^2 \cos\theta}{q^2 - \lambda\rho T(\rho)}, \tag{31}$$

for the density $\rho(s)$ and the tangent angle $\theta(s)$ which must be solved, in the absence of guides or rollers, subject to the boundary conditions

$$\left.\begin{array}{rcl} \rho(0) &=& \rho_j \\ \theta(0) &=& \theta_j \\ x(0) &=& x_j \\ y(0) &=& y_j \end{array}\right\}, \tag{32}$$

$$\left.\begin{array}{rcl} \rho(s_*) &=& \frac{q}{u_n} \\ \theta(s_*) &=& \theta_n \\ x(s_*) &=& x_n \\ y(s_*) &=& y_n \end{array}\right\}, \tag{33}$$

where $s_*$ is the unknown constant length of tow in the handling system.

In order to solve equations (30)-(33) for a general $E(\rho)$ we adopt a shooting method. We begin by making a guess for the unknown constants $q$, $\theta_j$, and $s_*$ and then numerically integrate the equations (30) and (31) from $s = 0$ to $s = s_*$. Next, we check if the constraints on density and nip position in equations (33) are satisfied to within a given tolerance, via equations (24) and (25). If they are then the problem is solved. If they are not then we make improved guesses for our three shooting parameters and repeat the integration.

In the presence of intermediate guides and rollers things become slightly more complicated.

# 4 Motion Over Guides, Nips and Rollers

We now incorporate the frictional forces encountered at the intermediate guides, nips, and rollers into the model. Each of these situations can be handled as a variation of the same basic problem, that being the motion of the tow band around a circular cylinder of radius $a$, which is rotating at angular velocity $\Omega$. Both $a$ and $\Omega$ being non-dimensional. See Figure 6. In addition to the forces already considered in section 3 there is now a tangential frictional

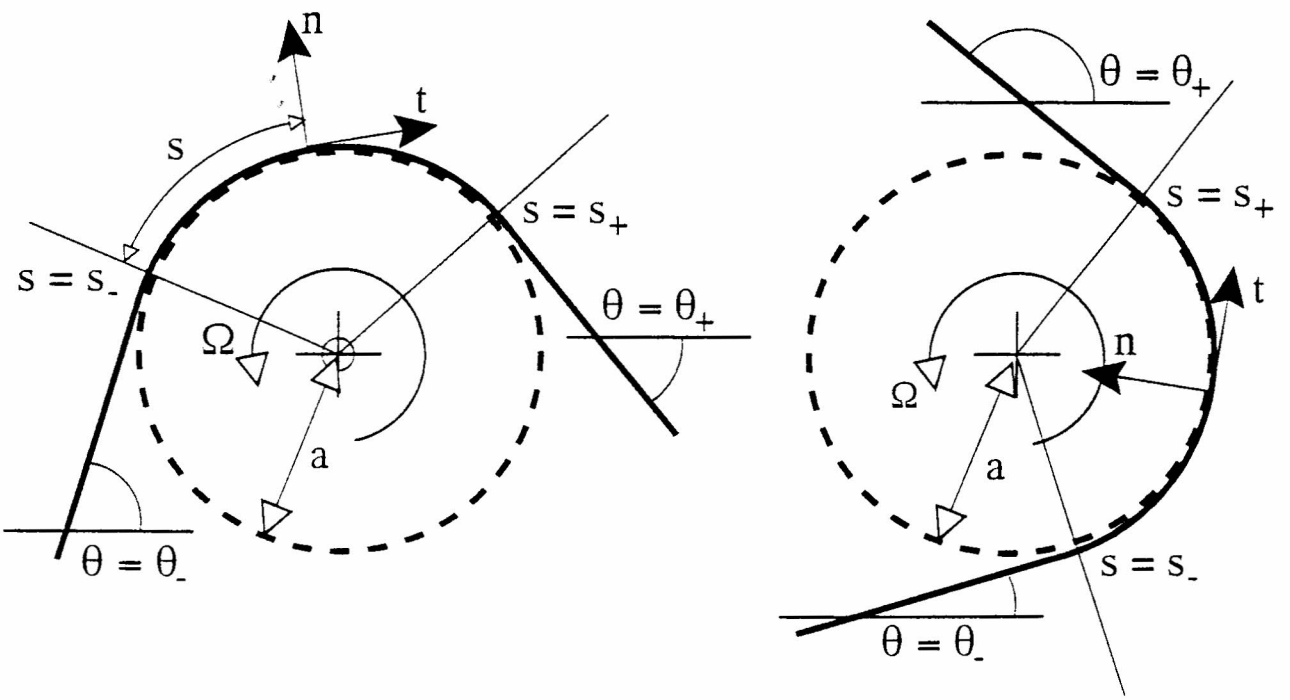


Figure 6: Motion of the tow band around a circular guide or roller of radius $a$ rotating with angular velocity $\Omega$. Notice that the normal reaction force is in the opposite direction with respect to the normal vector $\mathbf{n}$ if the tow band is wound anti-clockwise instead of clockwise.

force imparted to the tow by the cylinder whose magnitude is proportional to the normal reaction force of the cylinder on the tow band. Also, some simplifications can now be made to our existing model for tow dynamics due to the fact that the tow band shape is now known, The tow band shape is assumed to be that of the cylinder, and therefore no longer varies in time.

With these two points in mind the governing equations (17)-(19) can be rewritten in the form

$$\frac{\partial \rho}{\partial t} + u\frac{\partial \rho}{\partial s} + \rho\frac{\partial u}{\partial s} = 0, \tag{34}$$

$$\frac{\partial u}{\partial t} + u\frac{\partial u}{\partial s} = \frac{\lambda}{\rho}\frac{\partial T}{\partial s} - \gamma \sin\theta - \mu \operatorname{sgn}(u - V) N(s,t), \tag{35}$$

$$u^2\frac{d\theta}{ds} = \frac{\lambda T}{\rho}\frac{d\theta}{ds} - \gamma\cos\theta \pm N(s,t), \tag{36}$$

where $\mu$ is the coefficient of friction between the tow band and the cylinder, $V = \mp\Omega a$ is the tangential velocity of the roller at the point of contact, and $N(s,t)$ is the non-dimensional normal reaction force per unit mass of the cylinder on the tow band. The $+$ and $-$ signs above refer to cases where the tow band is wound either clockwise or anti-clockwise around the cylinder respectively.

With these definitions in place it is now possible to define the difference between a guide, a nip, and a roller. A guide is defined by the condition $V = 0$, a nip moves with specified speed $V$ and satisfies the additional boundary condition that $u = V$ at a given $\theta(s,t)$, and a roller is free to move at an unknown speed $V$ determined by the constraint that no overall torque is applied to the roller by the tow band.

Since $\theta(s)$ is in general given by the formula $\theta(s) = \theta_- \mp a^{-1}(s - s_-)$ , due to the circular shape of the cylinder, equation (36) can be rearranged to give the normal reaction force per unit mass $N(s,t)$ in the form

$$N(s,t) = \frac{1}{a\rho^2}\left(\lambda\rho T(\rho) - \rho^2 u^2\right) \pm \gamma\cos\theta. \tag{37}$$

As before we can then eliminate the tension $T(s,t)$ from equation (35) to give

$$\frac{\partial u}{\partial t} + u\frac{\partial u}{\partial s} = -\frac{\lambda E(\rho)}{\rho^3}\frac{\partial \rho}{\partial s} - \gamma\sin\theta - \mu\operatorname{sgn}(u - V) N(s,t), \tag{38}$$

We are then faced with the task of solving equations (34), (37), and (38) subject to suitable initial and boundary conditions on $\rho(s,t)$ and $u(s,t)$.

## 4.1 Steady Motion Over Guides, Nips, and Rollers

If we now consider the steady motion of a tow band over rotating circular cylinder of small radius some simplifications can be made to the above model. These assumptions not only allow us to treat the guide, nip, and roller positions as fixed points in space, as far as the

handling system as a whole is concerned, across which jump conditions can be applied but is also realistic as the guides and rollers in the actual handling system are of small radius compared with the typical length of the tow band shape.

The corresponding jump conditions are calculated by solving an ordinary differential equation which is valid on a shorter length scale of the cylinder surface. The approach is therefore entirely consistent. In order to derive the equations which hold on the cylinder surface we work with $\theta(s)$ as our independent variable instead of the arc length $s$ since the change in arc length across the cylinder is now of order $a \ll 1$ whereas the change in tangent angle remains of order unity.

If we make the assumptions mentioned above, the system of equations (34), (37), and (38) collapse into the ordinary differential equation

$$\frac{d\rho}{d\theta} = \pm\mu \operatorname{sgn}(u - V) \frac{(q^2 - \lambda\rho T(\rho))}{(q^2 - \lambda E(\rho))}, \tag{39}$$

where $q = \rho u$ is the non-dimensional, unknown, constant mass flow rate. This equation can be integrated, subject to the boundary condition $\theta = \theta_-$ when $\rho = \rho_-$, to provide a relationship between the jump in $\rho$ and the jump in $\theta$ across a given guide or roller. We are now in a position to consider the steady or unsteady motion of a tow band around an a handling system consisting of a J-box, a nip, and a number of intermediate guides and rollers.

# 5 Summary and suggestions

The main suggestion for the way forward with generating a two-dimensional model for the flow through the J-box is to use a plastic flow model, of the kind discussed in section 2.1.3. The simplest kind of model would be the incompressible rigid-plastic kind set out in section 2.1.3, but further developments to include compressibility along the lines of section 2.1.4 are likely to be needed in view of the nature of the material.

For modelling the tow-handling system, the existing Acordis model has been developed and extended in sections ? above.

A number of other suggestions and comments made during the study group are assembled here for completeness:

> If a high frequency modulation is superimposed on the main sweep of the plaiting arm, this would force the short wavelength scrumpling to be coherent across the width of the J-box. This might reduce the liability to tangling on exit.
>
> If the sweep of the plaiting arm sped up in accordance with the tow velocity, then a more even lay-down might be achieved without some of the short wavelength scrumpling. (Though the folding induced by the star-wheel crimper is inevitably present of course.)
>
> If the plaiting process is adjusted so as to deposit more tow on the inside of the bend (*ie* the side where $r$ is close to $a$) then this might counteract the tendency to form gap and tilt.

If the guide labelled G in Figure 1 were vibrated perpendicular to the tow plane, that might smooth out any stick-slip trouble in the pull-out process.

If a sensor (perhaps ultrasonic) could detect the exit bed angle, a suitable control system could govern small perturbations to the speed of the nip rollers (marked B in Figure 1) that determine the rate of pull-off. Such a control system should be able to maintain a horizontal tow bed in the exit duct by pulling off tow slightly faster for a time when an adverse tilt (as in Figure 2) develops.

# References

[1] The Mathematical Theory of Plasticity. R Hill. Oxford University Press, 1950.